Measurement 170 (2021) 108742

Contents lists available at ScienceDirect

Measurement

journal homepage: www.elsevier.com/locate/measurement

Frequency domain data merging in operational modal analysis based on least squares approach

Çağlayan Hızal

Department of Civil Engineering, Izmir Institute of Technology, Urla, Izmir, Turkey

ARTICLE INFO

Keywords:
Modal identification
Multi-setup data
Operational modal analysis
Data merging
Least squares approach
Mode shape assembly

ABSTRACT

Assembling of multi-setup measurements emerges as a challenging problem in the structural health monitoring applications and may cause some important issues in the estimation of global modal parameters such as frequency, damping ratio and modal shape vector. To overcome this problem, a novel frequency domain pre-identification data merging method is proposed in this study. In the proposed methodology, to obtain a single measurement set, a least squares approach is employed resulting in a global response that is scaled from the multi-setup data. For the verification of the proposed merging procedure, one numerical, two experimental studies and one real data application have been conducted. The results obtained from the numerical, experimental and real data analysis indicate that the presented methodology provides rather high-quality estimations for multi-setup measurement problems.

1. Introduction

Estimation of dynamic properties such as frequency, damping ratio and mode shape vectors has a crucial importance in the vibration based Structural Health Monitoring (SHM) of engineering structures. In this context, various Operational Modal Analysis (OMA) techniques, which do not require any input data, have been presented to the literature. Natural Excitation Technique and Eigensystem Realization Algorithm (NExT-ERA) [1], Stochastic Subspace Identification (SSI) [2], Frequency Domain Decomposition (FDD) [3] and Bayesian Operational Modal Analysis (BAYOMA) [4] come forward as best-known and widely implemented techniques in the literature. Although the effectiveness of the OMA methods has been validated by numerous studies, there are still some limitations in the application of these methods. Among these limitations, the multi-setup problem, which specifically may become a necessity in the SHM of large-scale structures, arises as an important challenge. In such a case, since each setup corresponds to an individual cluster, assembling those clusters may produce significant errors. Consequently, those errors can adversely affect the identification quality of modal parameters.

For modal frequencies and damping ratios, it is also possible to obtain a global value as the ensemble average of the local values evaluated at each setup. Estimation of a global mode shape vector, however, might be a much more challenging issue since the identified local mode shapes are confined to different locations of the measured structure. In general sense, two fundamental approaches emerge in the literature for the global mode shape vector estimation: (*i*) Post-identification mode shape assembly [5–10], and (*ii*) pre-identification data merging techniques [11–14]. The first one implements an assembly procedure to the local mode shape vectors identified at individual (or local) setups. The latter one is based on the merging of data acquired from the individual setups before the identification procedure.

One of the generic versions of the post-identification mode shape assembly techniques can be found in [13], which proposes a simple scaling procedure for local mode shapes. This procedure, however, requires a reference setup selection as a first step. Then, the local mode shapes obtained from the remaining setups are scaled with respect to the selected reference setup. This approach gives rather reasonable solutions when all measurement setups share constant reference points. In case of the roving reference sensor(s), however, significant issues can arise due to the error accumulation in the scaling sequences [15]. To overcome this problem, a global least squares approach which does not require any reference setup selection has been developed by Au [16]. The theory of global least squares approach is based on the minimization of equally weighted discrepancies between the local mode shapes and its counterparts of the global mode shape vector. The resulting algorithm leads to a high quality of estimation with considerably small error accumulation compared to the local least squares approach [15].

The least squares approaches do not consider the identification quality (or uncertainty) of the local mode shapes. Therefore, the

E-mail address: caglayanhizal@iyte.edu.tr.

https://doi.org/10.1016/j.measurement.2020.108742
Received 8 June 2020; Received in revised form 30 August 2020; Accepted 15 November 2020
Available online 20 November 2020

accuracy of the global least squares approach may significantly decrease in case the quality of the identified local mode shapes shows large fluctuations among different setups. From this perspective, Bayesian methods, which assemble the mode shapes by considering identification uncertainties, provides more precise and reasonable solutions for the multi-setup problems [5,6,8]. On the other hand, Bayesian methods are capable of quantifying a posterior uncertainty for the estimated global modal parameters [9,17]. Recent developments in this regard indicate that Bayesian techniques [5,6] also give more accurate results with respect to pre-identification methods in case of large variability in operational conditions (e.g. weakly excited modes in one or more setups). The reason for this difference lies in the fact that those methods are capable of estimating high quality mode shapes by incorporating the local modal parameters proportional to their second order statistical values (e.g. variance, coefficient of variation). However, despite this effectiveness, the post-identification techniques have an important disadvantage due to the remarkable increase in computational time and effort in case of the large number of measurement setups [18]. From this aspect, pre-identification methods might be more useful since they provide a fast modal identification process with a single measurement set.

Available pre-identification data merging techniques, generally implements a data-based assembly strategy using a specific OMA technique, such as [12,13]. Although reasonable results can be achieved for natural frequencies and damping ratios by those strategies, large amounts of errors can arise in the estimated mode shapes. To solve this problem, a refined procedure can be employed, which combines the deterministic SSI and Kalman filter applications, and provides more accurate results for mode shapes [19]. To manage uncertainty propagation in multi-setup applications, an extended version of SSI based data-merging technique has been proposed by [20]. A similar subspace-based data merging method is presented by Mevel et al. [11] considering the non-stationarity of input signals. In addition, a Power Spectral Density (PSD) based scaling procedure has been proposed by [21] to obtain a single data set from multi setup measurements. In this scaling procedure, the Fast Fourier Transform (FFT) of the measured data are synchronized by using a scaling factor that is calculated as a ratio of cross-spectral densities.

The most important disadvantage of pre-identification methods is that they are either being limited with a specific modal identification technique or require a scaling procedure based on a single [14] and/or constant reference Degree of Freedom (DoF) [21]. To obtain a more general and practical solution procedure for such kinds of multi-setup problems, a novel pre-identification methodology is introduced in this study. Motivated from the global least squares approach, an FFT based scaling procedure is employed to generate a global response data that reasonably matches with local measurements in the frequency-domain. The presented technique is not restricted to single reference DoF and works well for all possible reference sensor placement configurations (permanent or roving). To validate the proposed methodology, numerical, experimental and real data investigations are undertaken. According to the results obtained from the numerical and experimental studies, one can be concluded that the presented method provides rather reasonable solutions for multi-setup problems in case of large variations in the excitation levels.

2. Theory of the proposed data merging methodology

In SHM applications, it is generally not possible (and practical) to measure all DoFs of a structure due to the lack of instruments (e.g. acceleration sensors, data transmission cable and/or data acquisition device). Dynamic properties of the measured structure, however, can be estimated more accurately by increasing the number of measurement setups. In this context, the number of overall measured DoFs can be calculated as below:

$$N = \sum_{i}^{n_s} (n_i - r_i) \tag{1}$$

where n_s is the number of measurement setups, n_i is the number of DoFs measured at i^{th} setup, and r_i represents the number of reference measurement channels between the i^{th} and $(i\text{-}1)^{\text{th}}$ setups (when $i = 1$, $r_i = 0$). Using the scaled discrete FFT, the acceleration response vector acquired at the i^{th} setup can be written in the frequency domain as below, [15].

$$\ddot{\boldsymbol{Y}}_i(\omega_k) = \sqrt{\frac{\Delta t}{n_t}} \sum_{j=0}^{n_t-1} \ddot{\boldsymbol{y}}_i(t_j)\, e^{-i2\pi jk/n_t}; \qquad k = 1, \quad 2, \quad \ldots \quad , N_q \tag{2}$$

where $\ddot{\boldsymbol{y}}_i(t_j) = \ddot{\boldsymbol{y}}_i(t = j\Delta t)$ and $\ddot{\boldsymbol{Y}}_i(\omega_k) = \ddot{\boldsymbol{Y}}_i(\omega = k\Delta\omega)$ represent $n_i \times 1$ sized time and frequency domain acceleration responses and N_q is the ordinate of the Nyquist frequency [15]. Here, Δt, $\Delta\omega$ and n_t indicate the sampling time and frequency, and the number of samples, respectively. In addition, t and ω represent the continuous time and frequency variables while t_j and ω_k are that of the discrete time and excitation frequency ordinates. In case of all vibration modes are well separated, in the vicinity of n^{th} modal frequency, the expected value of $\ddot{\boldsymbol{Y}}_i(\omega_k)$ can be separated into two components as below [15]:

$$E\left[\ddot{\boldsymbol{Y}}_i(\omega_k)\right]_{\omega_k \to \omega_n} = \underbrace{\boldsymbol{\varphi}_{ni} s_{ni}(\omega_k) h_n(\omega_k)}_{\text{modal response}} + \underbrace{\boldsymbol{\varepsilon}_i(\omega_k)}_{\text{noise}} \tag{3}$$

where φ_{ni} is the $n_i \times 1$ sized local mode shape vector that confines the measured DoFs at i^{th} setup, $s_{ni}(\omega_k)$ is the discrete FFT of the modal excitation (scalar) for the i^{th} setup, and $\varepsilon_i(\omega_k)$ is the $n_i \times 1$ sized measurement noise vector. In addition, $h_n(\omega_k)$ represents the n^{th} modal transfer function which is defined by [15]:

$$h_n(\omega_k) = \left[\left(\frac{\omega_n}{\omega_k} \right)^2 - 1 + \boldsymbol{i} 2\xi_n \left(\frac{\omega_n}{\omega_k} \right) \right]^{-1} \tag{4}$$

If the prediction errors due to the implemented modal identification technique are neglected, the modal parameters, including mode shape vector, modal frequency and damping ratio can be assumed invariant among the individual measurement setups. The modal forcing levels, however, may show significant variance among different setups. Here, a global response vector is defined as below so as to cover the local data measured at individual setups with a reasonable convergence:

$$E\left[\ddot{\boldsymbol{X}}(\omega_k)\right]_{\omega_k \to \omega_n} = \boldsymbol{\Phi}_n s_n(\omega_k) h_n(\omega_k) + \boldsymbol{\varepsilon}(\omega_k) \tag{5}$$

where $\ddot{\mathbf{X}}(\omega_k)$ and Φ_n represent the $N \times 1$ sized global acceleration response and mode shape vectors, respectively. In addition, $s_n(\omega_k)$ and $\varepsilon(\omega_k)$ indicate the discrete FFT of the modal excitation (scalar) and $N \times 1$ sized noise vector for the expected global response, respectively. In general sense, when the measured structure is strongly excited by the modal forcing, it can be expected that Eqs. (3) and (5) are dominated by the modal response due to the negligibly small measurement noise [15]. Then, the resulting local and global accelerations can be approximately defined by:

$$E\left[\ddot{\boldsymbol{Y}}_i(\omega_k)\right]_{\omega_k \to \omega_n} \approx \boldsymbol{\varphi}_{ni} s_{ni}(\omega_k) h_n(\omega_k) \tag{6}$$

$$E\left[\ddot{\boldsymbol{X}}(\omega_k)\right]_{\omega_k \to \omega_n} \approx \boldsymbol{\Phi}_n s_n(\omega_k) h_n(\omega_k) \tag{7}$$

Thus, a relation can be defined between the local and global accelerations as follows:

$$\alpha_i(\omega_k) E\left[\ddot{\boldsymbol{Y}}_i(\omega_k)\right]_{\omega_k \to \omega_n} = \boldsymbol{L}_i E\left[\ddot{\boldsymbol{X}}(\omega_k)\right]_{\omega_k \to \omega_n} + \boldsymbol{e}_i(\omega_k) \tag{8}$$

which equivalent of:

$$\boldsymbol{\varphi}_{ni}\alpha_i(\omega_k)s_{ni}(\omega_k)h_n(\omega_k) = \boldsymbol{L}_i\boldsymbol{\Phi}_n s_n(\omega_k)h_n(\omega_k) + \boldsymbol{e}_i(\omega_k) \tag{9}$$

where $\mathbf{L}_i$ represents an $n_i \times N$ sized observation matrix which extracts the measured part of the global response, and $\alpha_i(\omega_k)$ indicates a scaling factor (scalar) to equalize the spectral density levels of $s_n(\omega_k)$ and $s_{ni}(\omega_k)$. In addition, $\mathbf{e}_i(\omega_k)$ represents an $N \times 1$ sized error vector.

As the excitation frequency $\omega_k$moves away from ω_n, the modal response can be assumed negligibly small in comparison to the noise term. Thus, in such a case, the expected values of $\ddot{\mathbf{Y}}_i(\omega_k)$ and $\ddot{\mathbf{X}}(\omega_k)$ can be defined as:

$$E\left[\ddot{\boldsymbol{Y}}_i(\omega_k)\right] \approx \boldsymbol{\varepsilon}_i(\omega_k) \tag{10}$$

$$E\left[\ddot{\boldsymbol{X}}(\omega_k)\right] \approx \boldsymbol{\varepsilon}(\omega_k) \tag{11}$$

Considering this assumption, Eq. (8) turns into the following form:

$$\alpha_i(\omega_k)\boldsymbol{\varepsilon}_i(\omega_k) = \boldsymbol{L}_i\boldsymbol{\varepsilon}(\omega_k) + \boldsymbol{e}_i(\omega_k) \tag{12}$$

Sensor noise sensitivity has an important role on the effectiveness and validity of the presented theory. For example, servo accelerometers produce considerably less channel noise (say about 1 $\mu g/Hz^{1/2}$) in comparison to piezo-electric accelerometers and Micro-Electro-Mechanical Sensors (MEMS) [15]. It can be deduced from the here that servo accelerometers give much smoother PSD spectrum with a larger signal-to-noise ratio (*snr*) and gives more accurate results for the presented methodology. On the other hand, such kind of channel noise not only may be induced by the installed accelerometers but also may stem from the data acquisition system (e.g. data acquisition device and/or data transmission cable). In this context, the resulting channel noise (or measurement noise) can be modeled as a stationary stochastic process [15]. From this perspective, it can be concluded that estimating the channel noise density is more possible compared to the modelling errors induced by unconsidered model parameters (e.g. closely spaced modes, heavy or non-classical damping, and non-stationary input excitation). A more comprehensive discussion in this regard can be found in [22]. Consequently, it can be stated that although a less channel noise density positively contributes to the effectiveness of the proposed methodology, the presented scaling process can still work with reasonably high channel noise. However, a large variability in the channel noise levels among different setups may cause significant errors in the presented scaling procedure.

In case of the measurement sensors have similar noise sensitivities without any additional biased errors due to the measurement system, and modelling errors are negligibly small, it can be expected that the channel noise densities are in the same levels at all setups. Consequently, the estimated global response can preserve the data quality of the local measurements not only within narrow bands but also at out of the resonant frequencies. Otherwise, noisy responses may be generated during the scaling procedure due to the modelling errors. Therefore, the following conditions should be satisfied in order to minimize those modelling errors.

- The measured response should contain well separated and strongly excited modes.
- The measured structure should be lightly damped and should be subjected to stationary input excitation.
- Channel noise spectral density levels should not show large variances among measurement setups.
- There should be at least one reference sensor, which does not coincide with a nodal point, at each setup.

Considering all of these aspects, a least squares equation can be defined to estimate a global acceleration response, as follows:

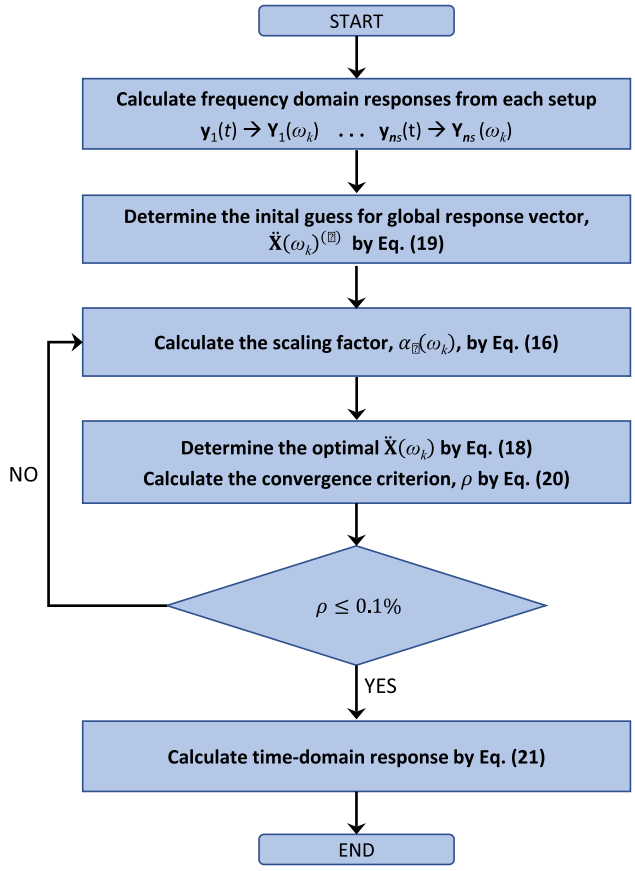

Fig. 1. Flowchart for the proposed data merging methodology.

$$J\left(\ddot{\boldsymbol{X}}, \alpha_i\right) = \sum_{i=1}^{n_s} \left\| \alpha_i(\omega_k)\ddot{\boldsymbol{Y}}_i(\omega_k) - \boldsymbol{L}_i\ddot{\boldsymbol{X}}(\omega_k) \right\|^2 \tag{13}$$

which can be extended as:

$$\begin{aligned} J\left(\ddot{\boldsymbol{X}}, \alpha_i\right) = \sum_{i=1}^{n_s} \Big\{ & \alpha_i^*(\omega_k)\alpha_i(\omega_k)\ddot{\boldsymbol{Y}}_i^*(\omega_k)\ddot{\boldsymbol{Y}}_i(\omega_k) - \alpha_i^*(\omega_k)\ddot{\boldsymbol{Y}}_i^*(\omega_k)\boldsymbol{L}_i\ddot{\boldsymbol{X}}(\omega_k) \\ & - \ddot{\boldsymbol{X}}^*(\omega)\boldsymbol{L}_i^T\alpha_i(\omega_k)\ddot{\boldsymbol{Y}}_i(\omega_k) + \ddot{\boldsymbol{X}}^*(\omega_k)\boldsymbol{L}_i^T\boldsymbol{L}_i\ddot{\boldsymbol{X}}(\omega_k) \Big\} \end{aligned} \tag{14}$$

Here, "*" denotes the complex conjugate and transpose. Thus, an optimal solution for $\alpha_i(\omega_k)$ and $\ddot{\mathbf{X}}(\omega_k)$ can be obtained by the gradient based minimization of Eq. (14). To this end, taking the first order gradient of Eq. (14) with respect to $\alpha_i^*(\omega_k)$ leads to:

$$\frac{\partial J}{\partial \alpha_i^*(\omega_k)} = \sum_{i=1}^{n_s} \left\{ \alpha_i(\omega_k)\ddot{\boldsymbol{Y}}_i^*(\omega_k)\ddot{\boldsymbol{Y}}_i(\omega_k) - \ddot{\boldsymbol{Y}}_i^*(\omega_k)\boldsymbol{L}_i\ddot{\boldsymbol{X}}(\omega_k) \right\} = 0 \tag{15}$$

Solving Eq. (15) for $\alpha_i(\omega_k)$ yields:

$$\widehat{\alpha}_i(\omega_k) = \frac{\ddot{\boldsymbol{Y}}_i^*(\omega_k)\boldsymbol{L}_i\ddot{\boldsymbol{X}}(\omega_k)}{\ddot{\boldsymbol{Y}}_i^*(\omega_k)\ddot{\boldsymbol{Y}}_i(\omega_k)} \tag{16}$$

Similarly, minimizing Eq. (14) with respect to $\ddot{\mathbf{X}}(\omega_k)$ gives:

$$\frac{\partial J}{\partial \ddot{\boldsymbol{X}}(\omega_k)} = \sum_{i=1}^{n_s} \left\{ -2\alpha_i^*(\omega_k)\ddot{\boldsymbol{Y}}_i^*(\omega_k)\boldsymbol{L}_i + 2\ddot{\boldsymbol{X}}^*(\omega_k)\boldsymbol{L}_i^T\boldsymbol{L}_i \right\} = 0 \tag{17}$$

Finally, the optimal value of the global response vector can be obtained as:

$$\widehat{\ddot{\boldsymbol{X}}}(\omega_k) = \frac{\sum_{i=1}^{n_s}\alpha_i(\omega_k)\boldsymbol{L}_i^T\ddot{\boldsymbol{Y}}_i(\omega_k)}{\sum_{i=1}^{n_s}\boldsymbol{L}_i^T\boldsymbol{L}_i} \tag{18}$$

Table 1
Sensor placement configurations in measurement setups.

Setup Number	Measured floors
1	1, 2, 3, 4
2	3, 4, 5, 6
3	5, 6, 7, 8
4	7, 8, 9, 10
5	9. 10, 11, 12

A flowchart is presented in Fig. 1 to summarize the overall procedure for the proposed methodology. Here, an iterative solution procedure is required to solve Eq. (13) since $\alpha_i(\omega_k)$ and $\ddot{\mathbf{X}}(\omega_k)$ are mutually dependent parameters. Therefore, the selection of an initial guess becomes necessary to initialize the iteration process. This initial guess can be evaluated by scaling the all local measurements with respect to a selected reference setup. However, such kind of a process enforces the global response and reference measurement setup to have the same spectral density, which may result biased errors. Therefore, a proper reference setup selection arises as an important issue in such a case. Instead, an initial guess can be determined by:

$$\ddot{\boldsymbol{X}}(\omega_k)^{(0)} = \frac{\sum_{i=1}^{n_s} \boldsymbol{L}_i^T \ddot{\boldsymbol{Y}}_i(\omega_k)}{\sum_{i=1}^{n_s} \boldsymbol{L}_i^T \boldsymbol{L}_i} \tag{19}$$

Subsequently, Eq. (13) can be solved iteratively until a prescribed convergence criterion is satisfied. Here, this convergence criterion is defined by:

$$\rho = \left| Re\left(\frac{\ddot{\boldsymbol{X}}^*(\omega_k)^{(j+1)} \ddot{\boldsymbol{X}}(\omega_k)^{(j)}}{\ddot{\boldsymbol{X}}^*(\omega_k)^{(j+1)} \ddot{\boldsymbol{X}}(\omega_k)^{(j+1)}} \right) - 1 \right| \times 100 \ (\%) \tag{20}$$

In this study, the upper limit of the convergence criterion is selected as 0.1%.

After obtaining the optimal $\ddot{\mathbf{X}}(\omega_k)$, a time domain global response can also be calculated by taking the inverse discrete Fast Fourier Transform (iFFT), as below [15].

$$\ddot{\boldsymbol{x}}(t_j) = \frac{1}{n_t} \sum_{k=0}^{n_t-1} \ddot{\boldsymbol{X}}(\omega_k) e^{i2\pi jk/n_t} \tag{21}$$

3. Numerical and experimental analysis

The performance of the presented frequency-based data merging methodology is investigated with one numerical, two experimental, and one real data examples. First, a numerical twelve story shear frame model, which has been previously analyzed by [5], is investigated.

Table 2
Identified natural frequencies (*Hz.*) for the first five modes.

Mode Number	Present study			Au and Zhang [5]	Analytical
	BFFTA	SSI-Cov	EFDD		
1	1.2648	1.2660	1.2686	1.2645	1.2635
2	3.7629	3.7659	3.7570	3.7652	3.7705
3	6.2209	6.2194	6.2211	6.2295	6.2185
4	8.5843	8.5794	8.5875	8.5717	8.5686
5	10.7908	10.7968	10.8320	10.7795	10.7827

Second, a ten-story laboratory model is experimentally analyzed in order to see the effects of constant and roving reference sensor placement configurations on the effectiveness of the proposed methodology. Finally, the presented method is implemented to a benchmark bridge which has been widely investigated in the literature.

3.1. Numerical analysis

In this section, a twelve-story shear frame structure is numerically modeled for analytical verification of the proposed data merging technique. In the numerical model, the considered structure has a uniform inter-story stiffness of $k = 4000\ kN/mm$ and a uniform mass of $m = 1000\ tons$. This numerical model was previously investigated by [5] for the validation of their Bayesian mode shape assembly technique. In the constructed model, each floor of the structure is subjected to independent and identically distributed (*i.i.d.*) Gaussian forces with a one-sided root spectral density of $19.6N/\sqrt{Hz}$. Acceleration responses at the floor levels are acquired in five measurement setups with 100 *Hz* sampling frequency. The sensor placement configurations for the employed measurement setups are presented in Table 1. In the generation of simulated data, each acquired acceleration response is contaminated by an *i.i.d.* Gaussian white noise with a one-sided root spectral density of $5\mu g/\sqrt{Hz}$.

The singular value spectra for the original (multi-setup) and the merged data are presented in Fig. 2. In the considered numerical model, all vibration modes are well separated. Therefore, only the maximum singular value spectra are shown for the original and the merged data. At first view, it is seen that the merged data shows a smooth spectrum as being compatible with that of the original data set. Since similar channel noises are assigned for each setup, any noise amplification and/or spurious mode effect triggered by the applied methodology are not visible on the presented spectrum for the merged data.

Three different identification techniques: Bayesian Fast Fourier Transform Approach (BFFTA), Covariance Driven Stochastic Subspace Identification (SSI-Cov), and Enhanced Frequency Domain

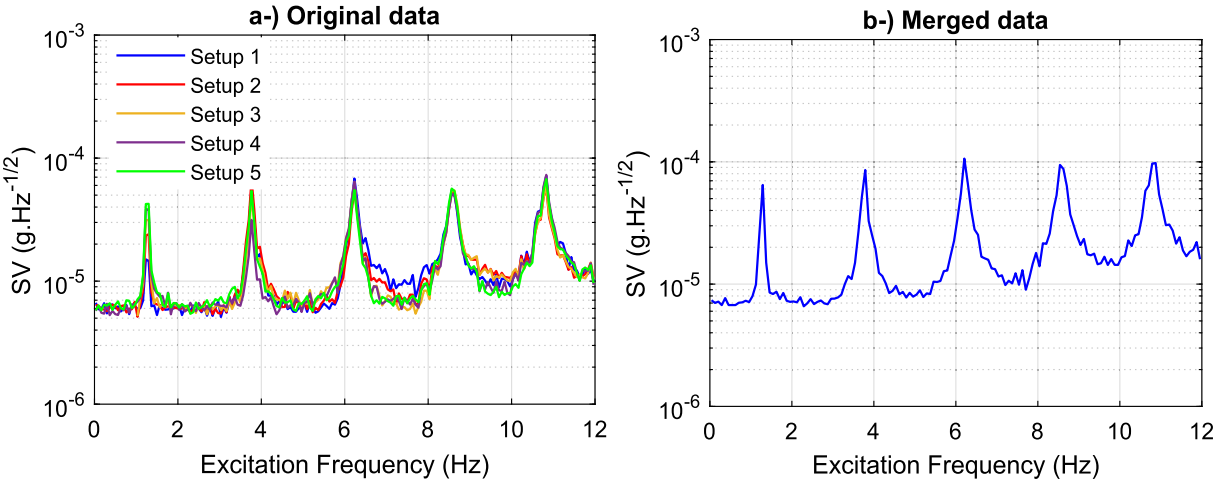

Fig. 2. Maximum singular value spectra: a-) original, and b-) merged data.

Table 3
Identified damping ratios (%) for the first five modes.

Mode Number	Present study			Au and Zhang [5]	Analytical
	BFFTA	SSI-Cov	EFDD		
1	0.94	1.10	1.51	0.91	1.00
2	0.94	1.03	0.76	1.05	1.00
3	1.00	0.94	0.78	1.02	1.00
4	0.97	0.94	0.93	1.07	1.00
5	0.96	0.91	0.69	1.06	1.00

Decomposition (EFDD) are employed for the simulated data. All these implementations are undertaken by using an in-house computer program coded by the author. Natural frequencies, damping ratios and modal shape vectors identified for the first five modes are presented in Table 2, Table 3 and Fig. 3, respectively. Here, the results reported by Au and Zhang [5] are also presented for comparison purposes. At first view, it is seen that the identification results are compatible with those presented by Au and Zhang [5]. Moreover, it is also observed that the obtained results perfectly match with the analytical values. Here, the major difference is observed in the damping ratios identified by EFDD. As it is known from the literature, EFDD provides less sensitive damping estimation when compared to BFFTA and SSI-Cov [23]. Therefore, this difference can be considered as reasonable for this numerical example.

3.2. Experimental analysis

For experimental verification, a comparative analysis which was undertaken using a ten-story laboratory shear frame model is presented in this section. In the conducted laboratory experiments, three piezoelectric accelerometers have been used which are defined with 1000 mV/g sensitivity and 11.4 $\mu g/\sqrt{Hz}$ spectral noise density. The measurement system consists of a laptop computer and a 16 channel USBDUX-Sigma data acquisition box with 24 bit analog to digital conversion and a constant current supply for the accelerometers [6]. The view of the laboratory structure and measurement system is presented in Fig. 4. Here, two different sensor placement scenarios namely Case-I and Case-II are considered in order to see the effects of roving and fixed reference sensor configurations on the accuracy of the proposed methodology. The sensor placements configurations for the considered scenarios are presented in Table 4. For each scenario, acceleration responses have been recorded in the weak direction of the structure with 100 Hz sampling frequency and 5 min duration.

The maximum singular value spectra of the original and the merged data obtained for Case I and II have been presented in Fig. 5 and Fig. 6, respectively. In the experimental procedure, acceleration responses of the structure have been measured under similar operational conditions for Case I and Case II. Therefore, the resulting singular value spectrums seem rather similar. The possible modes of the structure are detected near the frequencies of 2.6, 7.3, 11.7, 17.00 and 20.6 *Hz*. Some additional peaks also appear as structural modes around the frequencies of 15.5 and 23 Hz. However, these peaks do not correspond to any translational modes in the weak direction of the model structure. Therefore, these peaks can be considered as the possible modes of the laboratory structure in which the experimental study was conducted. In addition, a smooth singular value spectra are observed in the presented figures for the merged data, which follows a similar trend with the original data sets.

Similar to the numerical example presented in the previous section, three different operational modal analysis techniques, BFFTA, SSI-Cov and EFDD, have been implemented in this section. Additionally, a Bayesian Mode Assembly (BMSA) technique has been employed on the collected data for comparison purposes. The effectiveness of the implemented BMSA algorithm has been previously validated by [6]. Therefore, the results obtained by BMSA technique can be considered as reference values for this analysis. In this context, the identified natural frequencies and damping ratios obtained for Case I and II are presented in Tables 5 and 6, respectively. The identified modal shape vectors are

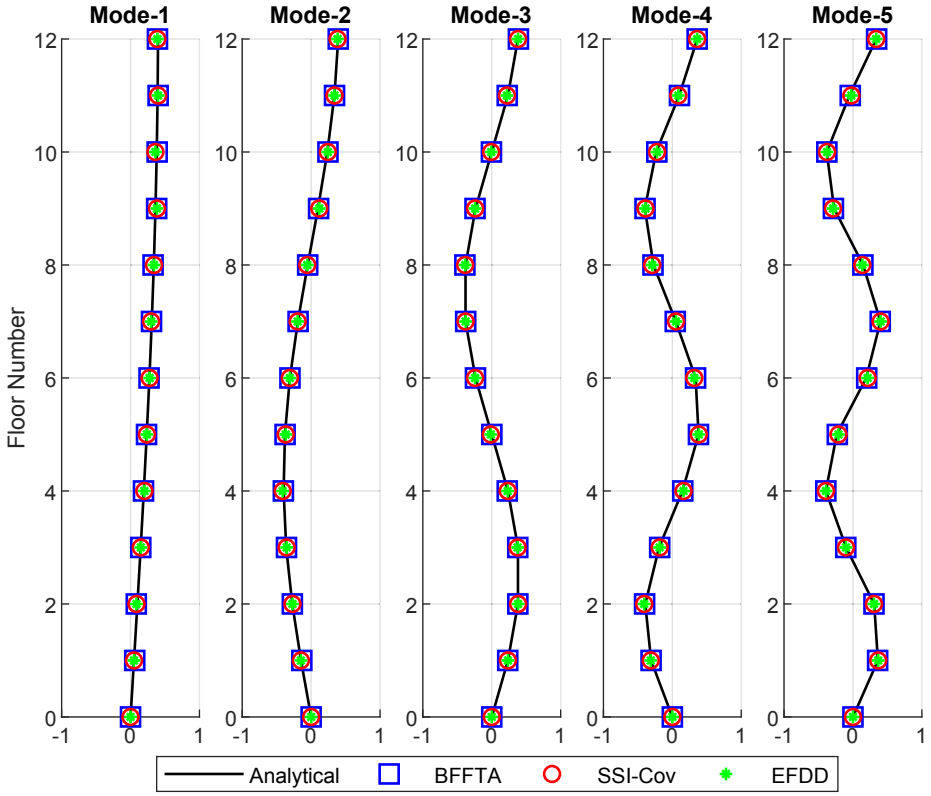

Fig. 3. Identified and analytical mode shapes.

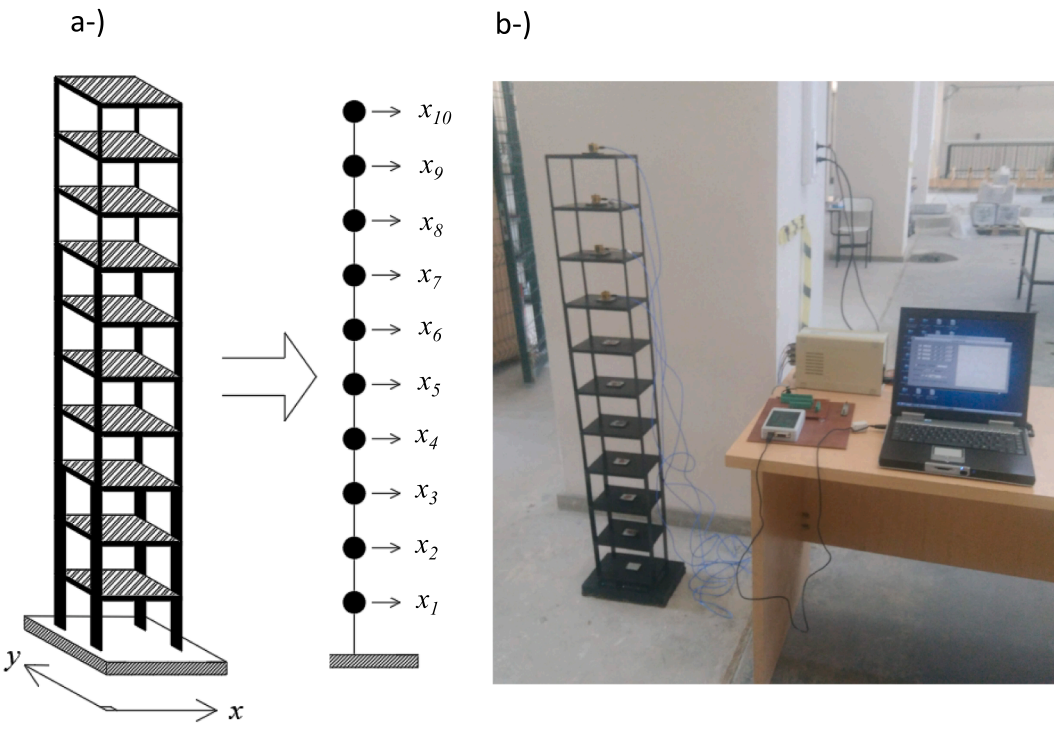

Fig. 4. a-) Schematic representation of the model structure, b-) experimental setup (reproduced from [6,24]).

Table 4
Sensor placement configurations in measurement setups.

Setup Number	Measured floors	
	Case I	Case II
1	1, 2, 3	1, 2, 10
2	3, 4, 5	3, 4, 10
3	5, 6, 7	5, 6, 10
4	7, 8, 9	7, 8, 10
5	9. 10	9. 10

shown in Fig. 7 and Fig. 8 as well. According to the presented results, it is observed that the presented merging procedure provides quite reasonable solutions for the implemented modal analysis methods. In addition, it can be deduced from here that the applied merging procedure also gives similar results for roving and permanent reference sensor configurations.

3.3. Benchmark study

A benchmark bridge which has been widely analyzed in the literature is investigated in this section. The investigated structure was formerly known as Z24 highway bridge, which connects the two towns of Utzenstorf and Koppigen in Switzerland. The schematic view of the Z24 bridge is presented in Fig. 9.

The Z24 Bridge was previously measured by KU LEUVEN Structural Mechanics division under ambient and forced vibration effects to perform various SHM applications for different damage scenarios, which are represented by totally eighteen measurement sets. At each set, totally nine measurement setups with constant reference sensors have been employed [25]. The schematic representation of the measurement setups is also shown in Fig. 9. Previously, numerous researches have

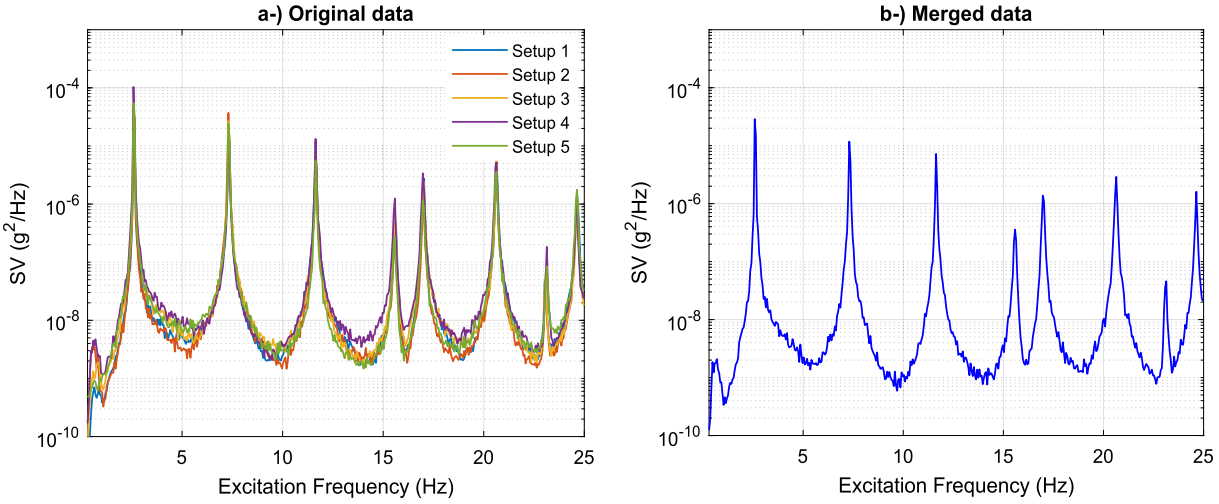

Fig. 5. Maximum singular value spectra for Case I: a-) original, and b-) merged data.

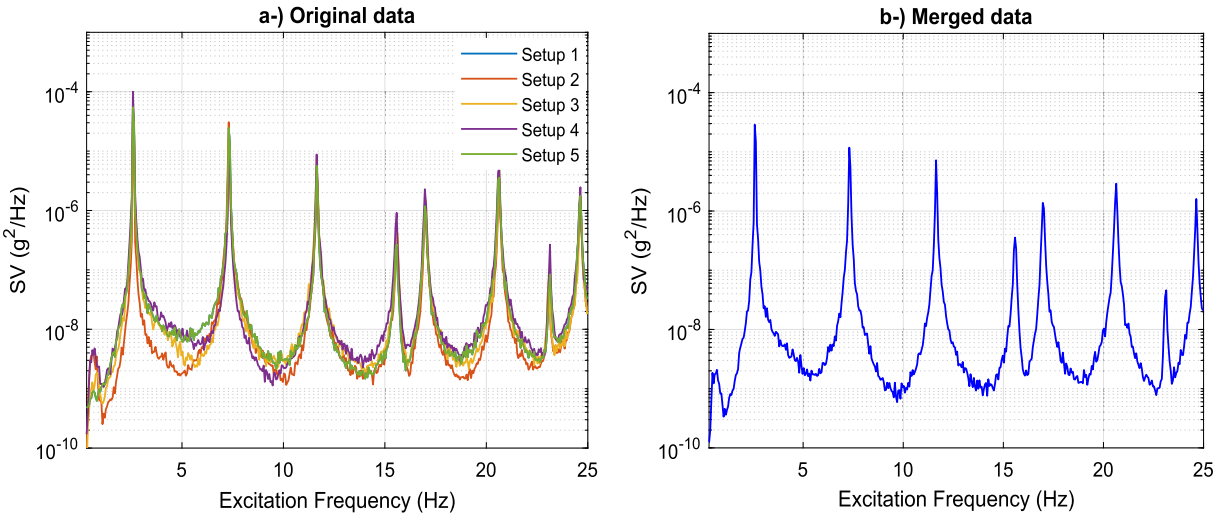

Fig. 6. Maximum singular value spectra for Case II: a-) original, and b-) merged data.

Table 5
Identified natural frequencies (*Hz*) obtained with roving and fixed reference sensor configurations.

Mode Number	BFFTA		SSI-Cov		EFDD		BMSA	
	Case I	Case II	Case I	Case II	Case I	Case II	Case I	Case II
1	2.608	2.609	2.607	2.608	2.606	2.612	2.610	2.610
2	7.318	7.320	7.318	7.321	7.335	7.331	7.323	7.323
3	11.648	11.649	11.642	11.648	11.658	11.658	11.649	11.649
4	16.994	16.993	16.992	16.991	16.992	16.975	16.996	16.996
5	20.627	20.630	20.629	20.629	20.643	20.641	20.627	20.626

Table 6
Identified damping ratios (%) obtained with roving and fixed reference sensor configurations.

Mode Number	BFFTA		SSI-Cov		EFDD		BMSA	
	Case I	Case II	Case I	Case II	Case I	Case II	Case I	Case II
1	0.23	0.22	0.23	0.22	0.30	0.25	0.20	0.20
2	0.21	0.22	0.23	0.24	0.33	0.34	0.19	0.19
3	0.17	0.16	0.16	0.16	0.17	0.18	0.19	0.19
4	0.23	0.23	0.20	0.22	0.22	0.23	0.22	0.22
5	0.17	0.19	0.16	0.18	0.18	0.16	0.14	0.14

been undertaken regarding the modal identification, finite element model updating and damage detection applications for the Z24 bridge [6,19,22,25–27].

The singular value spectra obtained for the original and the merged data are presented in Fig. 10. It is observed from here that the modal response in original data shows large variances among the local setups. In the presented figure, smooth modal response spectra and large *snr* levels are apparently visible for the lower modes. However, noisy plots appear starting from the fifth mode (around 12 Hz). In addition, one should be denoted that the channel noise levels show large variation among the measurement setups. Despite such a large variation, it is observed that the merged data provides a smooth spectrum in which the possible structural modes can be clearly detected. According to the presented spectrum for the merged data, the possible structural modes are visible around the frequencies of 3.80, 4.90, 9.70, 10.30, 12.50 and 13.00 *Hz*.

In the context of this application, BFFTA technique has been employed for modal parameter estimation. Here, the implemented modal identification technique, BFFTA, is capable of estimating PSD level of the modal excitation as well as the measurement noise. From this aspect, it might be more informative to show the variations in the PSD levels of the modal excitation and the measurement noise to understand how much the signal quality is influenced by the applied data merging strategy. For this purpose, the estimated PSD levels of the modal excitations and measurement noise are presented in Fig. 11. Here, it is observed that both PSD of modal excitation and measurement noise have a similar amount of decrease. It can be concluded from here that the applied methodology does not produce noisy data or spurious modes for the considered example. To the contrary, an amplification is observed in the *snr* levels up to the fourth mode. (see Fig. 10b).

Estimated modal parameters, including natural frequencies and damping ratios are presented in Table 7. For comparison purposes, the identification results reported by the previous researches undertaken for the Z24 bridge are provided as well. According to the presented results, a reasonable convergence is observed between the identified and the reference values, in which the relative difference remains less than 0.1% for the identified natural frequency values. Here, the largest relative difference (about 100%) appears in the fourth modal damping ratios.

The first sixth mode shapes of the Z24 bridge identified from the merged data are presented in Fig. 12. When they are compared to the results reported by previous researches, such as [6,22], it is seen that the estimated mode shapes are compatible with them. Here, the Modal Assurance Criterion (MAC) values between the identified mode shapes and the results reported by Hızal et al. [6] are calculated as 0.998, 0.995,

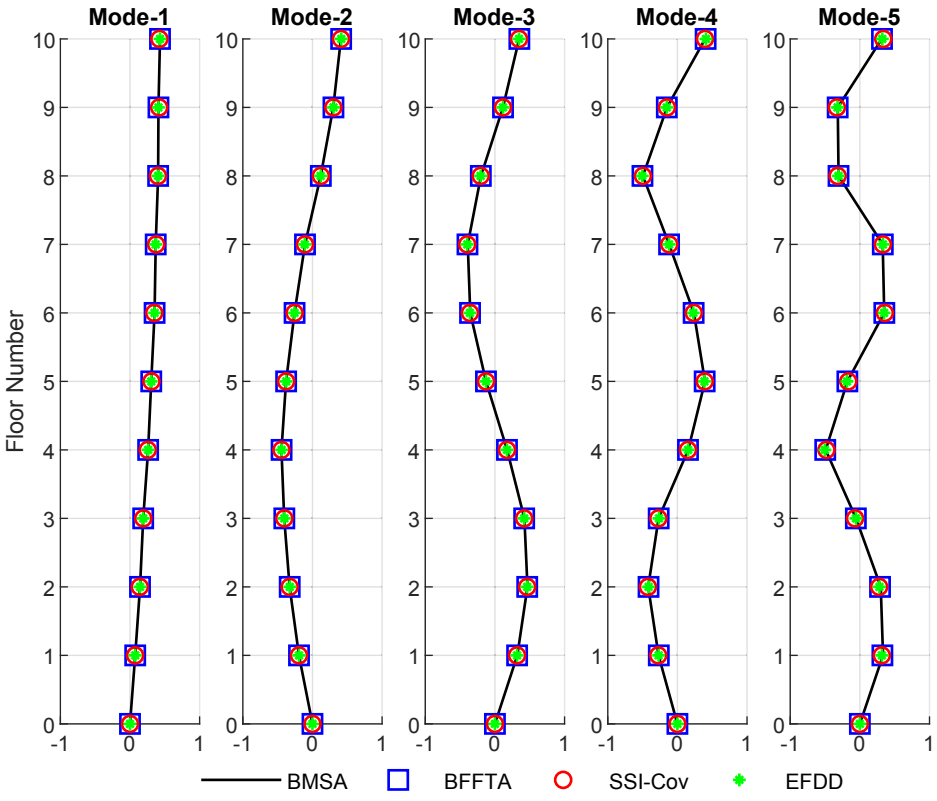

Fig. 7. Identified mode shapes for Case I.

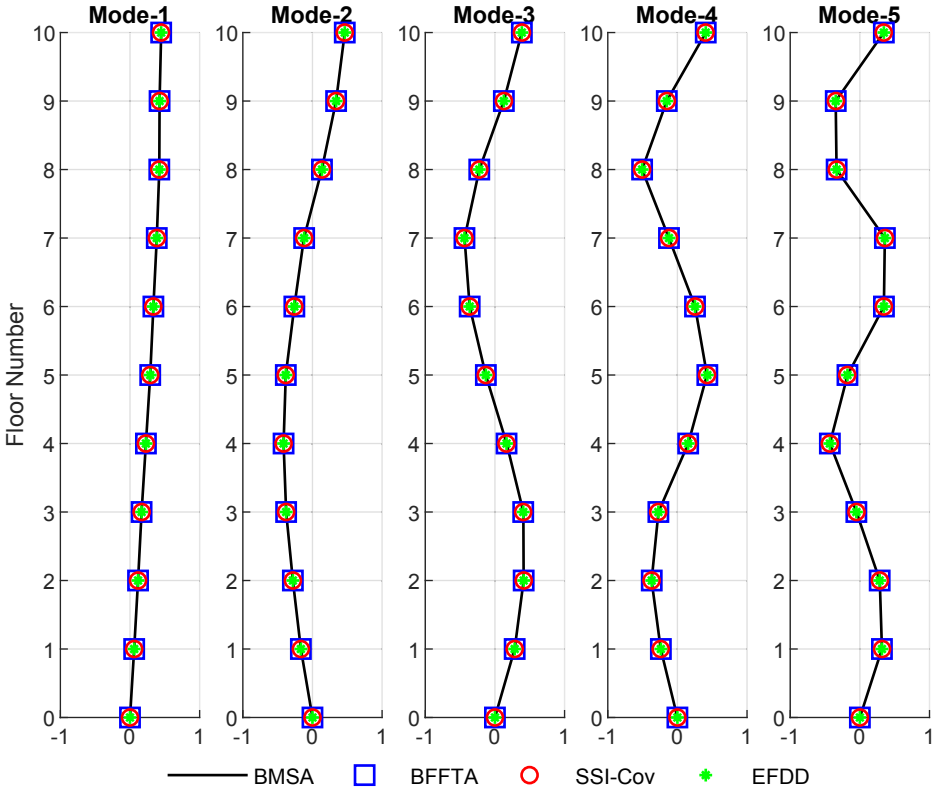

Fig. 8. Identified mode shapes for Case II.

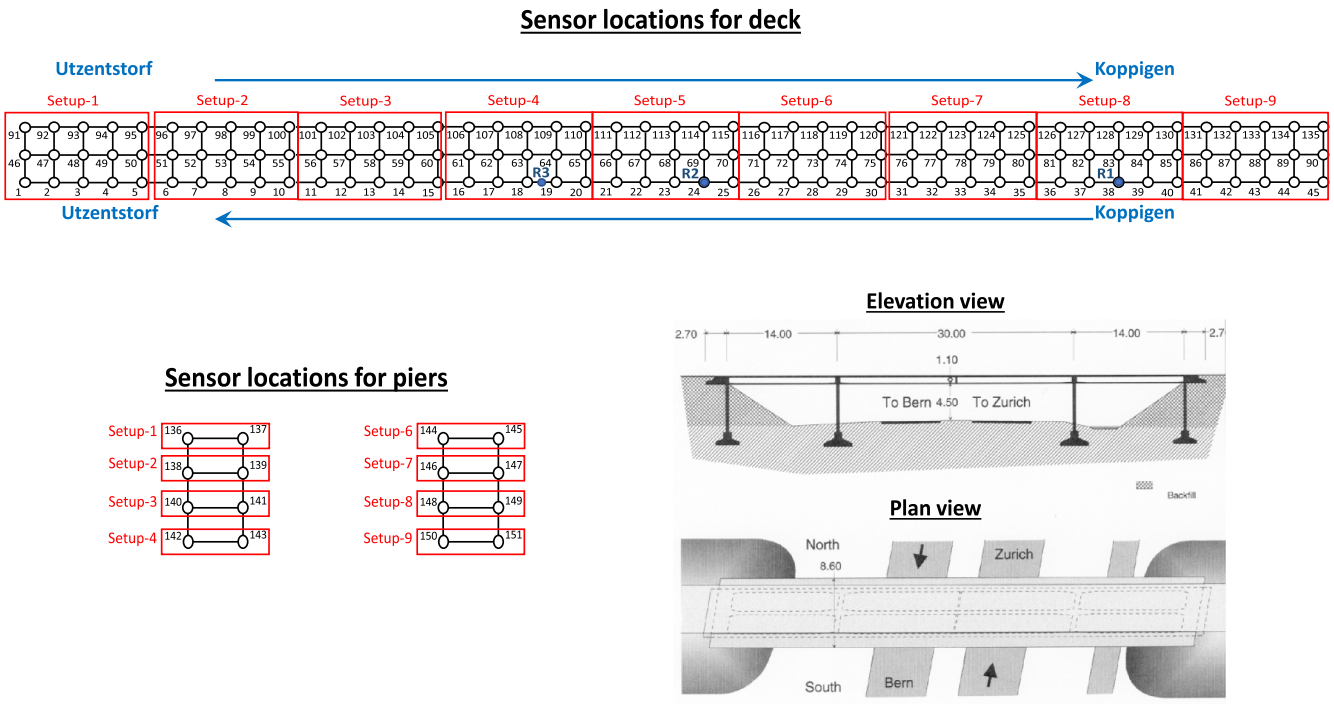

Fig. 9. Schematic view of the Z24 bridge and sensor placement configurations (Reproduced from [6]).

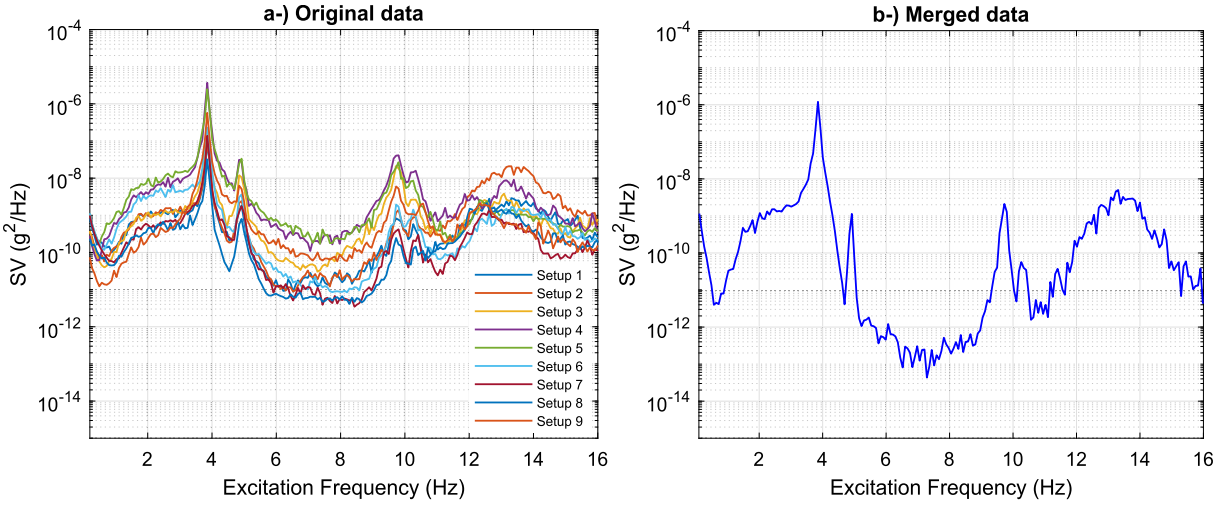

Fig. 10. Singular value spectrum obtained for a-) original, b-) merged data.

0.998, 0.999, 0.992, and 0.997, respectively.

4. Conclusions

In this study, a frequency-based data merging methodology is presented for multiple measurement sets. The underlying theory of the proposed methodology lies in a least-squares based scaling procedure based on the FFT data. The presented method is verified by one numerical and two experimental analysis, and one real data example. In this context, fundamental conclusions are summarized below.

- According to the obtained results, one can conclude that the presented merging methodology provides a large quality of data even for excitation levels that show significant variation among different setups. Based on the presented benchmark study, it is observed that the merged data provides a rather smooth spectrum, although the PSD of modal excitations shows up to approximately 100-fold variation among local measurement setups.
- When the modal *snr* values show a dramatic decrease (say $snr < 10$) in one or more measurement setups, the presented merging method may provide noisy data due to the loss of information of local data in the merging procedure. In such a case, most pre-identification data merging strategies may give unreasonable results. Post identification techniques such as BMSA, however, might be more effective for such kind of problems due to the fact that the uncertainty of local modal parameters is included in the assembly procedure.
- In the current SHM applications, it is also possible to minimize the channel noise in reasonable levels (say 1 – 10 $\mu g/\sqrt{Hz}$) by means of the technological developments in measurement systems. In such a case the presented method becomes quite practical provided that the

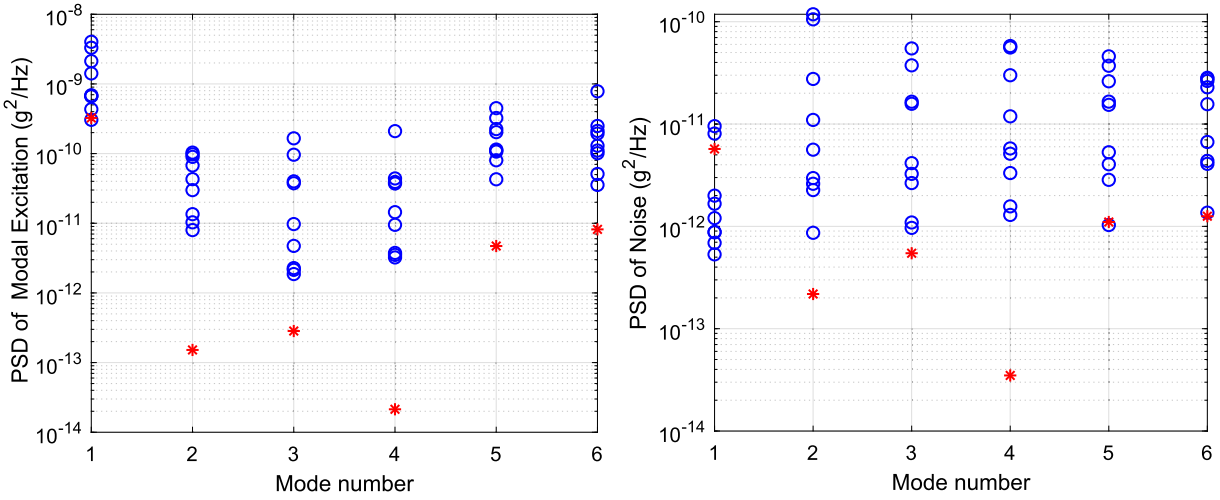

Fig. 11. Variation of identified PSD of modal excitation and noise for the multi setup (blue square) and the merged data (red star). (For interpretation of the references to colour in this figure legend, the reader is referred to the web version of this article.)

Table 7
Identified modal frequencies and damping ratios.

Mode Number	*f* (*Hz.*)				*ξ* (%)			
	Present Study	Peeters and Ventura [25]	Reynders et al. [26]	Hızal et al. [6]	Present Study	Peeters and Ventura [25]	Reynders et al. [26]	Hızal et al. [6]
1	3.86	3.86	3.86	3.85	0.87	0.90	0.80	0.92
2	4.90	4.90	4.90	4.89	1.43	1.40	1.40	1.36
3	9.74	9.77	9.76	9.77	1.01	1.30	1.40	1.19
4	10.30	10.30	10.30	10.32	0.95	1.40	1.30	1.94
5	12.59	12.50	12.42	12.53	2.51	2.50	2.80	3.18
6	13.29	13.20	13.22	13.22	2.29	3.30	3.40	3.05

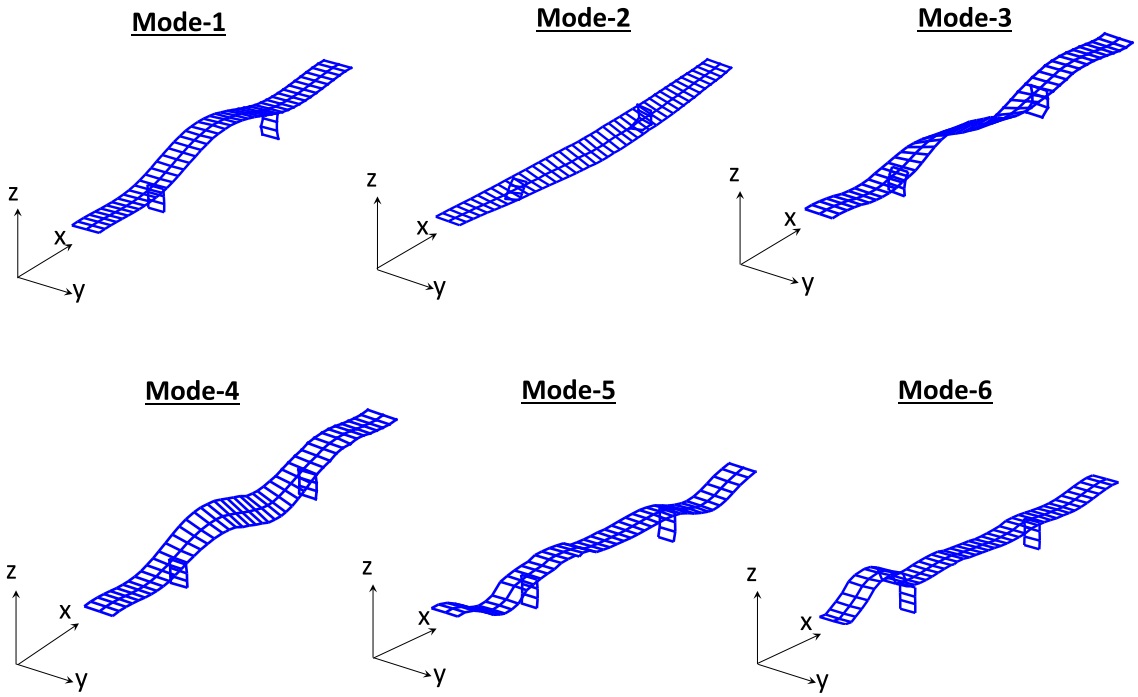

Fig. 12. Identified mode shapes for the Z24 bridge.

modelling assumptions are satisfied. Here, any modal identification technique (time or frequency domain) can be implemented for the merged data.

- In the presented methodology, the identification of local modal parameters at individual setups are not necessary since a single step identification procedure is performed using the merged data. Thus, in case of the large number of measurement setups, a significant decrease can also be obtained in the computational time and effort in comparison to the post-identification techniques.

Declaration of Competing Interest

The author declares that there is no known competing financial interests or personal relationships that could have appeared to influence the work reported in this paper.

Acknowledgements

The author would like to thank to KU LEUVEN Structural mechanics division for providing all the measurement data of the Z24 Bridge.

References

[1] J.M. Caicedo, Practical guidelines for the natural excitation technique (NExT) and the eigensystem realization algorithm (ERA) for modal identification using ambient vibration, Exp. Tech. 35 (2011) 52–58, https://doi.org/10.1111/j.1747-1567.2010.00643.x.

[2] P. Van Overschee, B. De Moor, Subspace algorithms for the stochastic identification problem, Automatica. 29 (1993) 649–660.

[3] R. Brincker, L. Zhang, P. Andersen, Modal identification of output-only systems using frequency domain decomposition, Smart Mater. Struct. 10 (2001) 441–445, https://doi.org/10.1088/0964-1726/10/3/303.

[4] K. Yuen, Bayesian Methods for Structural Dynamics and Civil Engineering, John Wiley & Sons (Asia) Pte Ltd, 2010.

[5] S.K. Au, F.L. Zhang, Fast Bayesian Ambient Modal Identification Incorporating Multiple Setups, J. Eng. Mech. 138 (2012) 800–815, https://doi.org/10.1061/(asce)em.1943-7889.0000385.

[6] Ç. Hızal, G. Turan, E. Aktaş, H. Ceylan, A mode shape assembly algorithm by using two stage Bayesian Fast Fourier Transform Approach, Mech. Syst. Signal Process. 134 (2019), 106328, https://doi.org/10.1016/j.ymssp.2019.106328.

[7] F.J. Cara, J. Juan, E. Alarcón, Estimating the modal parameters from multiple measurement setups using a joint state space model, Mech. Syst. Signal Process. 43 (2014) 171–191, https://doi.org/10.1016/j.ymssp.2013.09.012.

[8] W.J. Yan, L.S. Katafygiotis, A two-stage fast Bayesian spectral density approach for ambient modal analysis. Part II: Mode shape assembly and case studies, Mech. Syst. Signal Process. 54 (2015) 156–171, https://doi.org/10.1016/j.ymssp.2014.08.016.

[9] W. Yan, C. Papadimitriou, L.S. Katafygiotis, D. Chronopoulos, An analytical perspective on Bayesian uncertainty quantification and propagation in mode shape assembly, Mech. Syst. Signal Process. 135 (2020), 106376, https://doi.org/10.1016/j.ymssp.2019.106376.

[10] F. Zonzini, A. Girolami, L. De Marchi, A. Marzani, D. Brunelli, Cluster-based Vibration Analysis of Structures with Graph Signal Processing, IEEE Trans. Ind. Electron. 0046 (2020), https://doi.org/10.1109/tie.2020.2979563.

[11] L. Mevel, M. Basseville, A. Benveniste, M. Goursat, Merging sensor data from multiple measurement set-ups for non-stationary subspace-based modal analysis, J. Sound Vib. 249 (2002) 719–741, https://doi.org/10.1006/jsvi.2001.3880.

[12] M. Döhler, P. Andersen, L. Mevel, Data Merging for Multi-Setup Operational Modal Analysis with Data-Driven SSI, in: 28th Int. Modal Anal. Conf. Fr. Eur. HAL CCSD, Jacksonville, Florida USA, 2010.

[13] M. Döhler, E. Reynders, F. Magalhães, L. Mevel, G. De Roeck, Á. Cunha, Pre- and Post-identification Merging for Multi-Setup OMA with Covariance-Driven SSI, in: Dyn. Bridg. Vol. 5. Conf. Proc. Soc. Exp. Mech. Ser., Srpinger, Newyork, 2011: pp. 57–70. http://doi.org/10.1007/978-1-4419-9825-5_7.

[14] H. Ceylan, G. Turan, Ç. Hızal, Pre-Identification Data Merging for Multiple Setup Measurements with Roving References, Exp. Tech. 44 (2020) 435–456, https://doi.org/10.1007/s40799-020-00365-w.

[15] S.K. Au. Operational modal analysis: Modeling, Bayesian inference, uncertainty laws, Springer, Singapore, 2017, https://doi.org/10.1007/978-981-10-4118-1.

[16] S.K. Au, Assembling mode shapes by least squares, Mech. Syst. Signal Process. 25 (2011) 163–179, https://doi.org/10.1016/j.ymssp.2010.08.002.

[17] F.-L. Zhang, S.-K. Au, H.-F. Lam, Assessing uncertainty in operational modal analysis incorporating multiple setups using a Bayesian approach Feng-Liang, Struct. Control Heal. Monit. 22 (2015) 395–416, https://doi.org/10.1002/stc.1679.

[18] Ç. Hızal, Modal identification of structures by using Bayesian statistics, P.h.D. Dissertation, Izmir Institute of Technology, 2019.

[19] E. Reynders, G. De Roeck, Reference-based combined deterministic – stochastic subspace identification for experimental and operational modal analysis, Mech. Syst. Signal Process. 22 (2008) 617–637, https://doi.org/10.1016/j.ymssp.2007.09.004.

[20] M. Döhler, X. Lam, L. Mevel, Uncertainty quantification for modal parameters from stochastic subspace identification on, Mech. Syst. Signal Process. 36 (2013) 562–581, https://doi.org/10.1016/j.ymssp.2012.11.011.

[21] J.M.W. Brownjohn, Ambient vibration studies for system identification of tall buildings, Earthq. Eng. Struct. Dyn. 32 (2003) 71–95, https://doi.org/10.1002/eqe.215.

[22] Ç. Hızal, Modified frequency and spatial domain decomposition method based on maximum likelihood estimation, Eng. Struct. 224 (2020), 111007, https://doi.org/10.1016/j.engstruct.2020.111007.

[23] L. Zhang, T. Wang, Y. Tamura, A frequency-spatial domain decomposition (FSDD) method for operational modal analysis, Mech. Syst. Signal Process. 24 (2010) 1227–1239, https://doi.org/10.1016/j.ymssp.2009.10.024.

[24] Ç. Hızal, G. Turan, A two-stage Bayesian algorithm for finite element model updating by using ambient response data from multiple measurement setups, J. Sound Vib. 469 (2020), 115139, https://doi.org/10.1016/j.jsv.2019.115139.

[25] B. Peeters, C.E. Ventura, Comparative study of modal analysis techniques for bridge dynamic characteristics, Mech. Syst. Signal Process. 17 (2003) 965–988, https://doi.org/10.1006/mssp.2002.1568.

[26] E. Reynders, J. Houbrechts, G. De Roeck, Fully automated (operational) modal analysis, Mech. Syst. Signal Process. 29 (2012) 228–250, https://doi.org/10.1016/j.ymssp.2012.01.007.

[27] A. Teughels, G. De Roeck, Structural damage identification of the highway bridge Z24 by FE model updating, J. Sound Vib. 278 (2004) 589–610, https://doi.org/10.1016/j.jsv.2003.10.041.